

# Measurements of Ion Energization by a Pair of Beating Electrostatic Ion Cyclotron Waves

IEPC-2005-289

*Presented at the 29<sup>th</sup> International Electric Propulsion Conference, Princeton University*

*October 31 – November 4, 2005*

R. Spektor\* and Edgar Y. Choueiri†

*Electric Propulsion and Plasma Dynamics Laboratory (EPPDyL)*

*Princeton University, Princeton, New Jersey 08544*

**An experimental study of ion heating by beating electrostatic ion cyclotron (EIC) waves in a magnetized, rf-sustained plasma has been performed in order to explore an ion acceleration mechanism that was predicted theoretically. Ion heating up to 35% was observed in the presence of electrostatic waves excited by a two-plate antenna. It was found that ion-neutral collisions significantly alter dispersion properties of the backward branch of the EIC wave. In addition, it was shown that beating waves can heat ions to higher temperature than a single electrostatic wave. This enhancement in ion temperature was found to be 15% for the particular conditions of the reported experiment, but is expected to be significantly higher in a less collisional plasma. This finding supports theoretical prediction that beating waves can produce more efficient heating by interacting with ions below the single-wave velocity threshold.**

## Nomenclature

$v$	= velocity
$v_{ti}$	= ion thermal velocity
$\omega$	= wave frequency
$f_0$	= zero order particle velocity distribution function
$f_1$	= first order particle velocity distribution function
$n_0$	= zero order particle density
$n_1$	= first order particle density
$\kappa_{\perp}$	= perpendicular (to the magnetic field) wavenumber
$\kappa_{\parallel}$	= parallel (to the magnetic field) wavenumber
$\kappa_r$	= real component of $\kappa_{\perp}$
$\kappa_i$	= imaginary component of $\kappa_{\perp}$
$\omega_{ci}$	= ion cyclotron frequency
$\nu_{in}$	= ion-neutral collision frequency
$\nu_{ex}$	= ion-neutral charge-exchange collision frequency
$Q_{ex}$	= ion-neutral charge-exchange cross-section
$T_{i\perp}$	= perpendicular ion temperature
$T_e$	= electron temperature
$n_e$	= plasma number density
$V_{pp}$	= AC peak to peak voltage signal
$B$	= magnetic field
$P$	= neutral pressure

---

\*Graduate Student, Currently at the Aerospace Co. slava@rspektor.com

†Chief Scientist, EPPDyL. Associate Professor, Mechanical and Aerospace Engineering Department. Associated Faculty, Princeton Plasma Physics Laboratory, choueiri@princeton.edu.

## I. Introduction

Nonlinear wave particle interactions in plasmas occur naturally in many space physics problems, and are harnessed in the laboratory for plasma generation and plasma heating for fusion applications. The fundamental mechanism behind resonant type plasma heating with electrostatic waves was first elucidated theoretically by Karney<sup>1</sup> in 1977, who studied energization of a single magnetized charged particle with a single electrostatic wave (SEW). He found that the heating is inherently a stochastic mechanism and can only occur if the particle is above a resonance threshold ( $v \sim \omega/\kappa_{\perp}$ ), and the particle velocity is within a nonlinearly broadened resonance with the wave. In 1998 Benisti *et al.*<sup>2,3</sup> proposed an explanation of an ionospheric ion heating phenomenon, that relies on the nonlinear interaction between a pair of electrostatic waves and results in significant ion acceleration even for ions whose velocities are well below the single-wave threshold discussed by Karney. For this ion acceleration mechanism to occur they found that the following wave beating criterion must be satisfied

$$\omega_1 - \omega_2 = n\omega_{ci}.$$

where  $\omega_1$  and  $\omega_2$  are the frequencies of the two waves,  $\omega_{ci}$  is the ion cyclotron frequency, and  $n$  is a positive integer.

In a subsequent work<sup>4</sup> on the fundamental interaction between a single magnetized particle and a pair of beating electrostatic waves (BEW) we showed analytically and numerically that the above criterion is necessary but not sufficient. We also derived an additional criterion based on the Hamiltonian of the system, that needs to be satisfied for this mechanism to occur.

The main feature of the BEW ion acceleration is the lack of threshold for the initial ion velocity. This renders a plasma heating scheme based on this effect a particularly efficient one, as compared to resonant wave heating, since a larger portion of the ion distribution function can interact with the waves. Since the BEW ion acceleration mechanism can energize ions whose velocity is well below the single-wave threshold, we expect that in a real plasma the ion temperature will be enhanced, as compared to the case of SEW heating. This is particularly appealing for electric propulsion applications, where higher heating efficiency carries system benefits.

The predictions of the single-wave theory have been verified experimentally by the classic experiments of Skiff *et al.*<sup>5</sup> and other workers.<sup>6</sup> Our effort, reported here, is the first attempt to experimentally explore heating with beating electrostatic waves. Specifically, we measured the perpendicular ion temperature in a magnetized plasma in which either a single electrostatic (ES) wave, or a pair of beating ES waves were actively launched in an rf-sustained plasma. Unlike the single-wave experiment of Skiff *et al.*,<sup>5</sup> where a factor of 3.5 increase in ion temperature was observed, and ion-neutral collisions were negligible ( $\nu_{in}/\omega_{ci} \leq 0.02$ ), the presence of such collisions in our plasma required inclusion of their effects in the dispersion relation of the waves and resulted in a diminution of the level of heating.

The rest of the paper is organized as follows. Section II describes the experimental apparatus, diagnostics, and the antennas used to launch the electrostatic waves. Section III characterizes electrostatic wave propagation in a warm, rf-sustained plasma, and explores how ion-neutral collisions influence the wave dispersion properties. Section IV reports our observation of ion heating by a single *and* beating electrostatic waves, and section V contains some concluding remarks.

## II. Experimental Setup

The experiments were performed in the BWX magnetized, rf-sustained plasma discharge device, shown schematically in Fig. 1. The BWX vacuum chamber consists of a 6 cm diameter, 37 cm long Pyrex cylinder serving as the plasma source, connected through an aluminum plate to a 20 cm and 46 cm long Pyrex cylinder serving as a test section. The plasma is generated in the smaller cylinder by a helicon source (operated for these experiments in the inductive discharge mode) using a Boswell saddle-type rf antenna wrapped around the cylinder. The antenna is driven by an ENI 13.56 MHz 1.2 kW power supply. A power control circuit allows for pulsed as well as steady-state plasma generation. The vacuum chamber is placed inside an electromagnet, which produces a homogeneous, steady-state magnetic field up to 0.1 Tesla, that is uniformly axial throughout the test section.

The BWX experiment is typically operated with argon gas at 1 mTorr of neutral pressure. For the ion heating experiments the discharge was maintained by 125 watts of the rf power supplied to the helicon antenna, which produced plasma with a number density  $n_e \sim 10^{11} \text{ cm}^{-3}$ . The magnetic field was varied from 0.03 to 0.1 Tesla. The plasma in the BWX apparatus was characterized in details in Refs. [7] and [8]. For the experiments reported here the background electron and ion(perpendicular) temperatures were  $T_e = 3 \text{ eV}$  and  $T_{i\perp} = 0.11 \text{ eV}$ , and the ratio of the ion-neutral charge-exchange collision frequency to the ion cyclotron frequency  $\nu_{ex}/\omega_{ci} = 0.2$ , as will be shown in the next section. It should be noted that this ratio is an order of magnitude above that of the Skiff's experiment.<sup>5</sup>

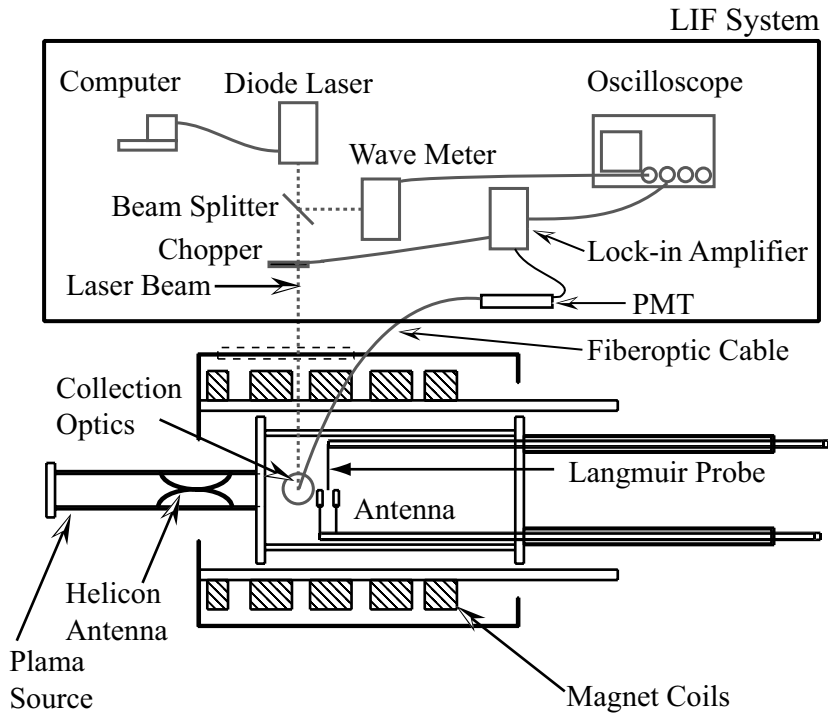


**Figure 1.** Schematic of the BWX experimental apparatus showing the vacuum chamber, magnet, helicon and two-plate antennas, and a Langmuir probe. The schematic also includes the LIF system that was used to measure the perpendicular ion velocity distribution function.

Electrostatic waves were launched into the plasma from either a two-plate or a loop antenna, which are described in details in the following sections. The signal to the ES antennas was generated by Wavetek 180 signal generators, which are able to produce up to 20 V<sub>pp</sub> signal into a 50Ω load. The signal was then amplified by an ENI 2100L broadband amplifier, and sent through a tuning circuit to match the ES antenna impedance. Schematics of the driving circuits for both ES antennas are shown in Figs. 3 and 5.

### A. Diagnostics

Two types of diagnostics were employed in the course of the experiments. A set of Langmuir probes measured plasma density  $n_e$ , electron temperature  $T_e$ , and wave dispersion properties. The probes were attached to a movable arm that allowed axial as well as rotational degrees of freedom. A schematic illustrating a Langmuir probe inside the BWX vacuum chamber is shown in Fig. 1.

Perpendicular ion velocity distribution was measured with a portable LIF system, which is also shown schematically in Fig. 1. The system consists of a 15 mW Sacher Lasertechnik Lynx tunable diode laser in Littrow configuration, which is set to 668.61 nm center wavelength to match an argon metastable transition line. The laser beam is modulated by a SRS SR-540 chopper spinning at approximately 3.5 kHz. A 10/90 beam splitter allows a Burleigh WA-1500 wavemeter to measure the wavelength of the laser beam with an accuracy of 0.2 ppm. Collection optics focuses the 442.7 nm emission light into an optical fiber which carries the signal to a Hamamatsu HC124-06MOD photomultiplier. A Stanford Research Systems SR830 lock-in amplifier further amplifies the photomultiplier signal with the chopper signal used as the reference. The LIF system can be used to measure steady-state as well as time-resolved ion velocity distribution.

### B. Two-plate Antenna

The two-plate antenna used to launch electrostatic waves is constructed from two 1 cm × 6 cm molybdenum plates placed ~3 cm apart along the magnetic field lines. The plates are oriented such that the long side and the surface normal are perpendicular to the magnetic field, as shown in Fig. 2. The plates are attached to a movable arm that can

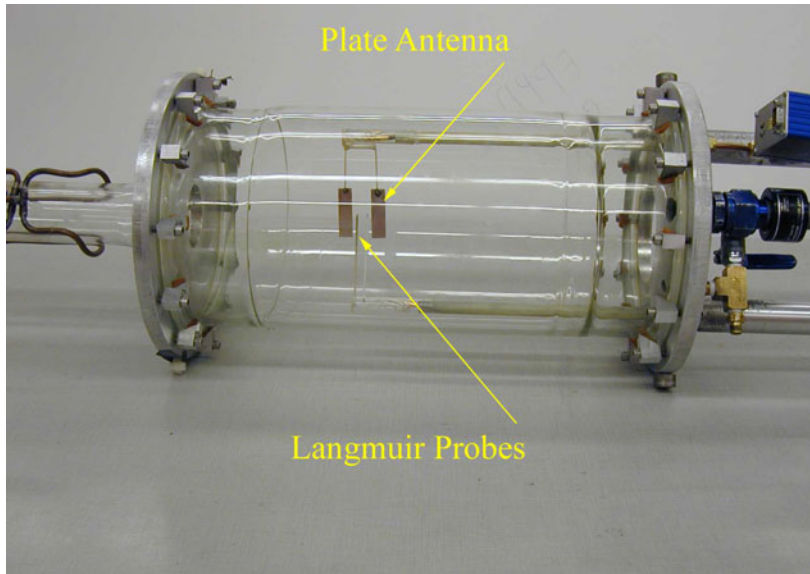


Figure 2. Photograph of the BWX test section showing the two-plate antenna attached to the moving arm. A set of Langmuir probes attached to the other arm can also be seen.

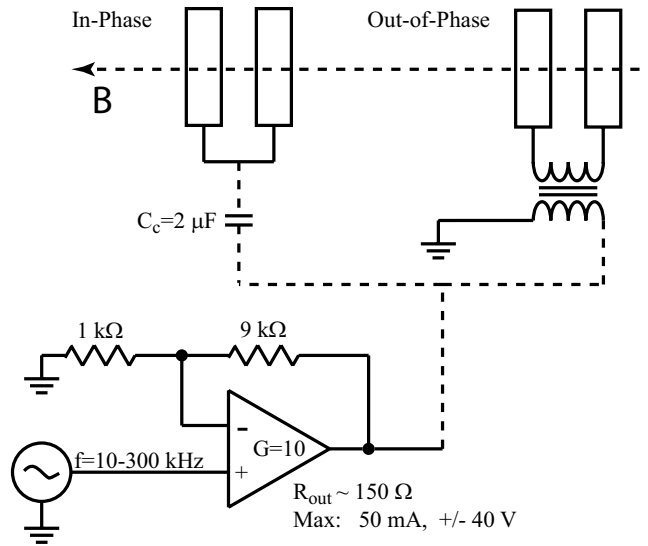


Figure 3. Circuit diagram of the two-plate antenna, signal generator, and rf amplifier. The two antenna plates can be driven in or out of phase by connecting them to the amplifier through either a capacitor or transformer.

rotate the antenna in and out of plasma column, and is also free to move along the axis of the vacuum chamber. The plates could be driven in or out of phase with each other by a circuit schematically illustrated in Fig. 3. When the plates are driven out of phase, the parallel wavenumber is controlled by the plate spacing, and when the plates are driven in phase, the parallel wavelength is controlled by the distance between the antenna and a conducting surface of the vacuum chamber. The waves launched by this two-plate antenna are characterized in details in our earlier paper.<sup>8</sup>

### C. Loop Antenna

In some experiments the loop antenna, shown in Fig. 4, was used. It was constructed from four aluminum rings measuring 1 cm wide and 6.7 cm in diameter each. The rings are attached to an arm, similar to the two-plate antenna, so that the entire antenna assembly can be rotated in and out of plasma, and moved along the axis of the experiment. To prevent the ohmic losses each loop was wrapped in Kapton tape. The antenna is inserted into the plasma such that the center axis of all four rings is coincident with the direction of the magnetic field. The spacing between the center of each loop is 3 cm. Just as with the two-plate antenna, loop spacing controls the parallel wavenumber,  $\kappa_{\parallel}$ , while the perpendicular wavenumber,  $\kappa_{\perp}$ , is free to evolve according to the dispersion relation as a function of wave frequency and other relevant plasma parameters.

While each ring can be supplied with a voltage signal independently, the two useful configurations are  $[0, \pi, 0, \pi]$ , and  $[0, \pi, \pi, 0]$ , as described in Ref. [9]. The first configuration establishes parallel wavenumber  $k_{\parallel} = 6 \text{ cm}^{-1}$  ( $\lambda \sim 1 \text{ cm}$ ), while the second configuration establishes a larger wavenumber  $k_{\parallel} = 12 \text{ cm}^{-1}$  ( $\lambda \sim 0.5 \text{ cm}$ ). In the experiments reported in this paper the loop antenna assembly was driven in the  $[0, \pi, 0, \pi]$  configuration. Experiments with the  $[0, \pi, \pi, 0]$  configuration produced similar results. A schematic of the electric circuit used to drive the loop antenna is illustrated in Fig. 5. Note that the turns ratio on the transformer is chosen to optimize the impedance matching between the ENI 2100L amplifier and the antenna.

## III. Electrostatic Wave Propagation in the BWX

Linear electrostatic dispersion relation for a homogenous and infinite plasma with finite temperature, can be derived from the Vlasov equation by including the BGK collision term as described by Choueiri<sup>10,11</sup>

$$-i(\omega - k_z v_z - k_{\perp} v_{\perp} \cos \theta + i\nu) f_1 + \omega_c \frac{\partial f_1}{\partial \theta} = \frac{iq}{m} \mathbf{k} \Phi \cdot \nabla_v f_0 + \nu \frac{n_1}{n_0} f_0, \quad (1)$$

where  $f_0$ ,  $n_0$ ,  $f_1$ , and  $n_1$  are zero and first order perpendicular ion velocity distribution functions and particle densities respectively,  $\theta$  is the angle between the wave propagation and magnetic field, and  $\Phi$  is the electric potential. After some manipulations the first order distribution function can be expressed as

$$f_1 = \frac{q}{T} f_0 \sum_n \sum_m \frac{J_n\left(\frac{k_{\perp} v_{\perp}}{\omega_c}\right) J_m\left(\frac{k_{\perp} v_{\perp}}{\omega_c}\right) e^{i(n-m)\theta}}{w + i\nu - n\omega_c - k_z v_z} \left[ (k_z v_z + n\omega_c) \Phi + i\nu \frac{n_1}{n_0} \frac{T}{q} \right]. \quad (2)$$

The equation above can be integrated over velocity space to obtain  $n_1$ , and used in the Poisson equation to yield the dispersion relation

$$1 + \sum_s \alpha_s \frac{1 + e^{-\mu_s} \xi_{0s} \sum_n I_n(\mu_s) Z(\xi_{ns})}{1 + i(\nu_s/k_z v_{ts}) e^{-\mu_s} \sum_n I_n(\mu_s) Z(\xi_{ns})} = 0, \quad (3)$$

where subscript  $s$  refers to the type of the charged species,  $\alpha_s = 1/k^2 \lambda_{Ds}^2$ ,  $\lambda_{Ds}$  is the Debye length,  $\mu = k_{\perp}^2 v_{\perp}^2 / 2\omega_c$ , and  $I_n(\mu)$  is the modified Bessel function of the first kind. It could be easily checked that upon setting  $\nu_s$  to zero, Eq. (3) reduces to the familiar collisionless electrostatic dispersion relation, e.g. Eq. (85) given by Stix in Ref. [12].

According to Eq. (3), two wave modes can propagate in the neighborhood of the ion cyclotron frequency. The first mode is a forward branch of the EIC wave ( $\omega/k_{\perp}$  parallel to  $\partial\omega/\partial k_{\perp}$ ) with a relatively large wavelength ( $\lambda \sim 6 \text{ cm}$ ). The other mode is the backward branch of the EIC wave ( $\omega/k_{\perp}$  antiparallel to  $\partial\omega/\partial k_{\perp}$ ) with the wavelength on the order of the ion Larmor radius. The latter branch is also sometimes referred to as the Neutralized Ion Bernstein Wave (NIBW). Figure 6(a) shows solutions to Eq. (3) for electrostatic waves in the frequency range of  $1-5\omega_{ci}$  for the plasma parameters typical in the BWX experiment, but neglecting collisions. The forward EIC and four branches of the NIBW waves are shown in this figure by thick lines. The line with the short dashes shows the imaginary part of the perpendicular wavenumber for the forward EIC branch. This wave is weakly damped. On the other hand, the lines

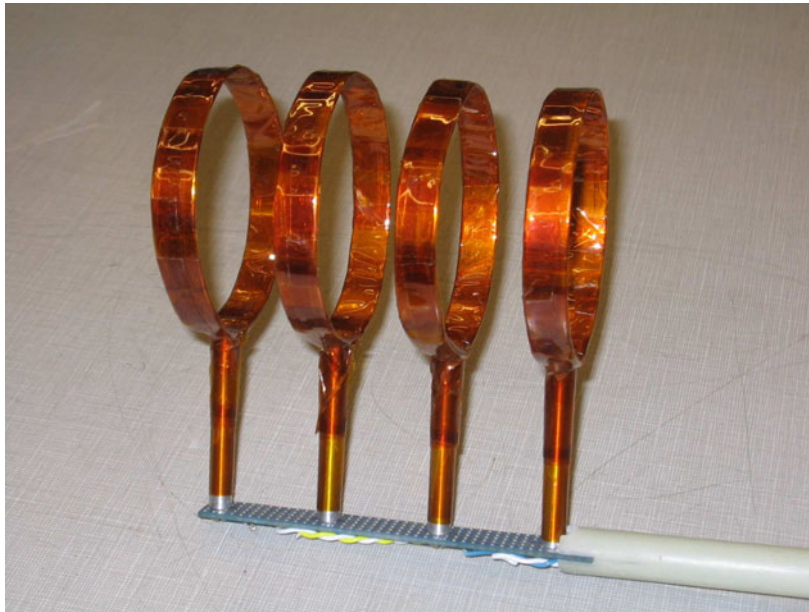


Figure 4. Photograph of the loop antenna showing its four aluminum rings. The rings are insulated from the plasma by wrapping them in Kapton tape.

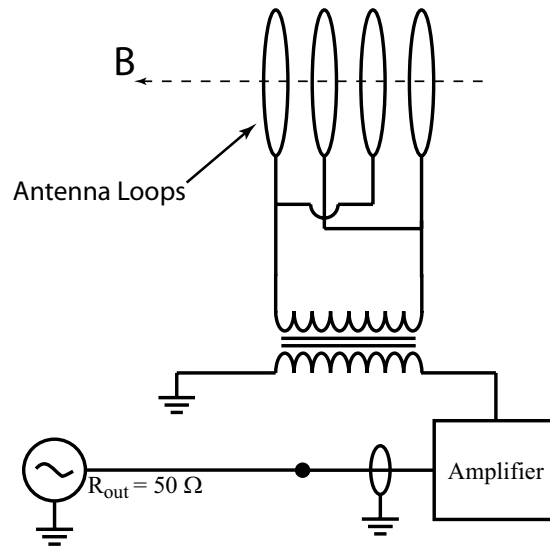


Figure 5. Circuit diagram of the loop antenna, signal generator, and rf amplifier. The rings are driven by a signal generator through an rf amplifier in either  $[0, \pi, 0, \pi]$  (shown here) or  $[0, \pi, \pi, 0]$  configuration. The transformer turns ratio is chosen to optimize impedance matching between the antenna and the driving circuit.

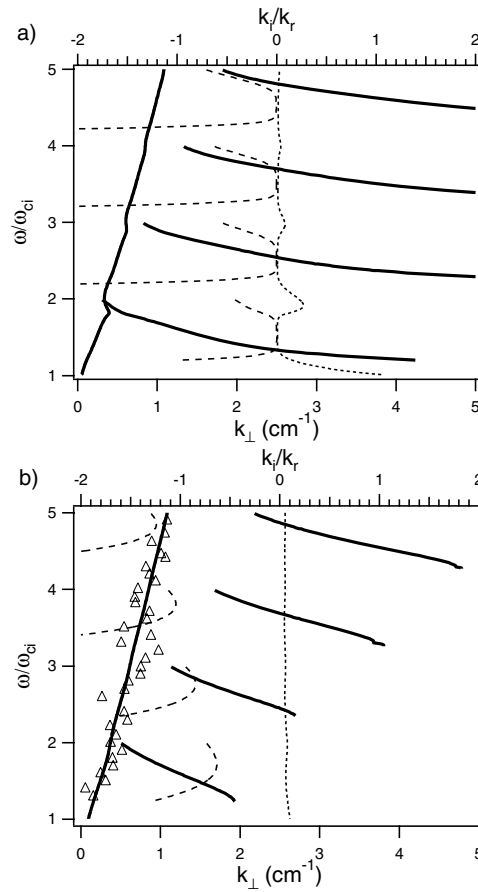
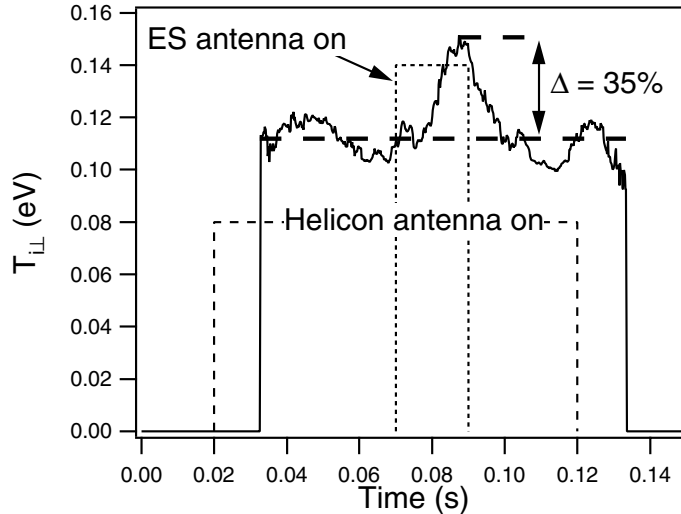


Figure 6. Electrostatic dispersion relation for waves propagating in an argon plasma slightly above the ion cyclotron frequency obtained from Eq. (3) for a) collisionless plasma, b) a plasma typical to the BWX experiment, including ion-neutral collisions at P=1 mtorr. The thick black lines show the wave frequency as a function of the real component of the wavenumber, while the dashed lines show the wave frequency as a function of the imaginary component of the wavenumber (top scale). Other plasma parameters common to both a) and b) are  $B=271$  G,  $T_e=3$  eV,  $T_{i\perp}=0.11$ , and  $\kappa_{\parallel}=0.14$  cm $^{-1}$ .

with the longer dashes represent the imaginary part of the wavenumber for the NIBW. A large negative imaginary component close to the wave harmonics indicates that this wave is highly damped at the exact resonances. However, away from the resonance  $k_i/k_r \ll 1$  and the wave can propagate away from the antenna. Indeed both the forward and backward branches of the EIC wave have been observed by Skiff *et al.*,<sup>5</sup> Alba *et al.*,<sup>6</sup> Goree,<sup>13</sup> and others in discharges with low neutral density ( $\nu_{in}/\omega_{ci} \leq 0.02$ ). As described in our earlier paper,<sup>8</sup> only the forward branch of the EIC wave could be detected in the BWX machine with our diagnostic method.

As we discussed earlier, the effect of ion-neutral charge-exchange collisions can be investigated by including the BGK collisional operator into the dispersion relation given by Eq. (3). For argon, at temperatures and densities typical to the BWX experiment, the charge-exchange collision cross-section is  $Q_{ex} \sim 10^{-14}$  cm $^2$ .<sup>14</sup> Charge-exchange collision frequency can be calculated as  $\nu_{ex} = Q_{ex}n_e v_{ti} \sim 1.5 \times 10^4$  s $^{-1}$ , where  $v_{ti}$  is the ion thermal velocity. With this collision frequency the ratio  $\nu_{ex}/\omega_{ci} = 0.2$ , which is an order of magnitude above that of the Skiff's experiment.

When ion-neutral charge-exchange collisions are taken into account, the dispersion relation shows that the backward branch becomes highly damped at all frequencies. Figure 6(b) shows the electrostatic dispersion that includes ion-neutral collisions. While the forward branch of the EIC wave is mainly unaffected, the imaginary component of the NIBW grows significantly. For example, with  $\omega/\omega_{ci} = 1.5$  the imaginary part of the wavenumber  $k_i$  increases by three orders of magnitude to  $k_i \sim k_r$ , as compared to the collisionless case. Thus, for our collisional plasma we expect the backward branch of the EIC wave to be damped within a short distance away from the antenna. It should be noted that Fig. 6(b) is obtained for an argon plasma typical to the BWX experiment at neutral pressure of 1 mTorr.



**Figure 7.** Ion temperature evolution for a 100 ms plasma pulse. A steady-state plasma is established at  $t \sim +15$  ms after the rf power is applied to the helicon antenna. Perpendicular ion temperature increases by  $\sim 35\%$  when an electrostatic wave propagates from the two-plate antenna. When the two-plate antenna is turned off the ion temperature returns to its ambient level.

Other plasma parameters common to both panels of Fig. 6 are  $B=271$  G,  $k_{\parallel}=0.14$  cm $^{-1}$ ,  $T_e=3$  eV, and  $T_{i\perp}=0.11$ . The experimental dispersion relation, shown in Fig. 6(b) by triangles, is in a good agreement with the forward branch of the EIC wave. As was mentioned above, we did not observe the backward branch of the EIC wave.

#### IV. Ion Heating in the BWX

The NIBW mode interacts with ions much stronger than the forward branch of the EIC wave, because its wavelength is on the order of the ion Larmor radius. Therefore, to observe any significant ion heating by an electrostatic wave in a warm, dense discharge, either the amount of power to the antenna or the magnetic field should be increased. The former increases the amount of power transferred from the waves to the ions. The latter decreases the ratio  $\nu_{in}/\omega_{ci}$ , thus making the plasma less collisional. Magnetic field in the BWX experiment is limited by the amount of current available from the magnet power supply. To reduce  $\nu_{in}/\omega_{ci}$  to an acceptable level the magnetic field should be increased to at least 0.3 T, which is three times the amount available. Therefore, we have chosen the route of increasing the power by amplifying the signal to the ES antenna. We have observed ion heating with the two-plate and the loop antennas. The heating with the two-plate antenna was more significant than heating with the loop antenna because more power could be transferred to the former than the latter.

We first performed a time-resolved study of ion heating by a single electrostatic wave launched by the two-plate antenna. For this study all plasma parameters were similar to the experiments described in Refs. [15] and [16]. Plasma was created by sending a 100 ms, 125W rf pulse to the helicon antenna. The two-plate antenna was turned on for 20 ms with a delay of 50 ms (to ensure that the plasma has reached a steady state), as shown in Fig. 7 by the dashed boxes. For the first 15 ms after the helicon antenna was turned on we observed a population of fast ions propagating through the plasma column. The velocity distribution of this population was found not to be Maxwellian, and thus the perpendicular ion temperature could not be established. Plasma reached a steady state after about 15 ms with an average temperature of 0.11 eV, shown by the thick dashed horizontal line in Fig. 7. The uncertainty in the temperature measurement can be determined from the temperature fluctuation when the two-plate antenna is off. Analysis shows that this error is  $\sim 0.01$  eV or 10%. We have also confirmed this uncertainty through a series of repeated steady-state ion temperature measurements with the two-plate antenna turned off.

When the ES antenna was turned on, we observed significant rise in the ion temperature. Figure 7 shows a 35% temperature increase. This increase is an order of magnitude below the ion heating reported by Skiff *et al.*<sup>5</sup> in a collisionless plasma, but on the same order as reported by Kline *et al.*<sup>17,18</sup> in an rf-sustained plasma. This is not surprising since we expect ion-neutral collisions to play an important role in wave damping.

Ion heating was observed within only a short distance away from the two-plate antenna. While the position of the

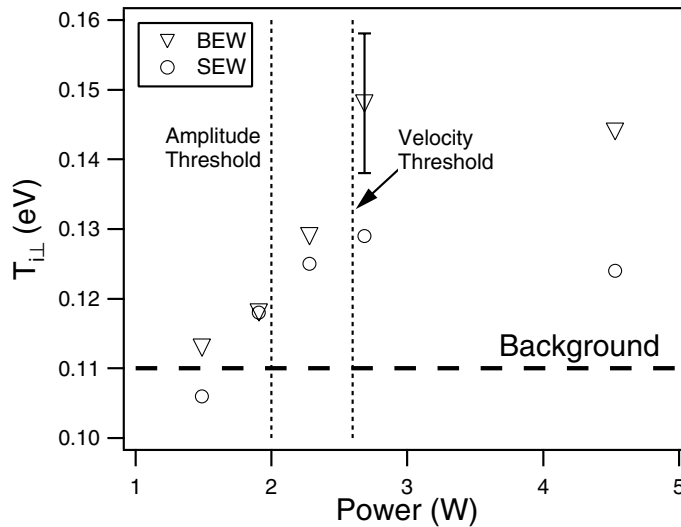


**Figure 8.** Results of the BEW ( $\nabla$ ) and SEW ( $\circ$ ) ion heating experiments. The background perpendicular ion temperature is 0.11 eV and is shown by the thick dashed line. The plot shows a heating threshold in wave power (amplitude) at about 2 watts above which there is significant heating for both BEW and SEW schemes. The data also indicates a threshold at about 2.5 watts above which the perpendicular ion temperature is higher for BEW heating.

antenna relative to the LIF measurement volume could not be precisely controlled, we observed a sharp increase in the ion temperature as the ES antenna was moved within half a centimeter of the LIF laser beam. This observation supports prediction of the collisional dispersion relation in Fig. 6b. The observed heating may be due to the backward branch of the EIC wave, but because this wave is highly damped we only observed heating very close to the antenna.

Next, we performed a study of the beating wave ion heating in a steady-state plasma. Time-resolved measurements are quite time consuming; it takes about 30 minutes to obtain a time-resolved ion temperature profile with 31 different wavelengths. In addition, a small drift in the helicon antenna tuning may change plasma parameters over this period. This renders time-resolved measurements impractical for comparison between different scans. On the other hand, a measurement of a steady-state plasma with 300 different wavelengths can be performed under 30 seconds. For this experiment we have compared ion heating by a single electrostatic wave with  $\omega = 3.5\omega_{ci}$  to that resulting from two beating waves with  $\omega_1 = 3.5\omega_{ci}$  and  $\omega_2 = 4.5\omega_{ci}$ . To ensure that the comparison is valid we set the total power for both beating waves to be the same as that for the single wave. Figure 8 shows the results of these experiments. Each data point is an average of three measurements.

Experiments revealed a threshold in the wave power (amplitude) at about 2 watts, above which there is a significant ion heating for both single and beating waves, as shown in Fig. 8. The threshold is observed by monitoring ion temperature as a function of power supplied to the antenna. Power was calculated by simultaneous measurements of oscillating current and voltage delivered to the antenna by the amplifier. A similar threshold was predicted by Karney *et al.*,<sup>19</sup> and observed by Skiff *et al.*<sup>5</sup> for a single electrostatic wave.

In our previous papers<sup>4,11,20,21</sup> we've shown that beating waves have the potential of providing a more "efficient" method of ion heating because they can interact with ions below this single-wave threshold. We expect that a wave interacting with a larger number of ions will be able to produce higher ion temperature. Figure 8 shows that above 2.5 watts there is a consistent increase in temperature resulting from the BEW heating compared to that of SEW, within the error bars of the measurements. We found that the increase in perpendicular ion temperature is  $\sim 15\%$  for the particular conditions reported in this paper. This provides the first qualitative evidence of an increase in efficiency between SEW and BEW heating. We expect that this enhancement would be much more significant without the effects of collisions. Collisions play two major roles, one is the damping of the electrostatic wave amplitude, as we discussed in the previous section, and the other is in changing the dynamics of the heating mechanism itself, as we discussed in Ref. [21].

The loop antenna could not be coupled to the plasma as well as the two-plate antenna. As the result the heating produced by the antenna was significantly smaller. We have attempted to heat ions with either a single or beating waves at frequencies varying from 30 kHz up to 1.8 MHz. We were able to heat ions by  $\sim 15\%$  with a wave at 450

kHz, and by  $\sim 2.4\%$  at 1.8 MHz. It is interesting to note that at this frequency ion heating most likely results indirectly from interaction between the lower-hybrid waves and electrons. Nevertheless, beating waves with  $\omega_1 = 1.77$  MHz and  $\omega_2 = 1.8$  MHz produced  $\sim 5\%$  heating, which is twice the heating produced by the single wave at 1.8 MHz.

## V. Final Remarks

In this paper we reported on an experimental investigation of ion heating by a single and beating electrostatic waves in an rf-sustained plasma in order to explore the heating enhancement predicted by the theory of ion acceleration by beating electrostatic waves. As a part of this study we have also investigated the electrostatic wave propagation, and effects of the ion-neutral charge-exchange collisions using the electrostatic dispersion relation, and shown that the backward branch of the EIC wave is strongly damped by these collisions.

We were able to produce ion heating with a single and beating waves using two different ES antennas. Using the two-plate antenna we were able to increase ion temperature by  $\sim 35\%$ . We observed a threshold behavior for both single and beating wave heating by increasing power to the ES antenna. In addition, we showed that beating waves can consistently heat ions to higher temperature than a single wave within the error bar of the measurement. This enhancement in ion temperature was found to be 15% for the particular conditions of these experiments, but is expected to be significantly higher in a less collisional plasma. This observation supports theoretical prediction that the beating electrostatic waves interact with ions moving below the single-wave velocity threshold.

## Acknowledgements

This work was supported by a research contract from the Air Force Office of Scientific Research (AFOSR), Department of Aerospace and Materials Science (Dr. Mitat Birkan, Program Manager). The authors would like to thank Bob Sorenson for providing his invaluable expertise with the rf circuitry and with constructing the experiment. The authors would also like to thank professor Earl Scime and Costel Biloiu of the West Virginia University for their help in designing and constructing the portable LIF system used in the experiments reported in this paper. This work was also supported by the Program in Plasma Science and Technology, Princeton Plasma Physics Laboratory.

## References

- <sup>1</sup>Karney, C. and Bers, A., "Stochastic ion heating by a perpendicularly propagating electrostatic wave." *Phys. Rev. Lett.*, Vol. 39, 1977, pp. 550.
- <sup>2</sup>Benisti, D., Ram, A., and Bers, A., "Ion dynamics in multiple electrostatic waves in a magnetized plasma. I. Coherent acceleration," *Phys. Plasma*, Vol. 5, No. 9, September 1998, pp. 3224.
- <sup>3</sup>Benisti, D., Ram, A., and Bers, A., "Ion dynamics in multiple electrostatic waves in a magnetized plasma. II. Enhancement of the acceleration," *Phys. Plasma*, Vol. 5, No. 9, September 1998, pp. 3233.
- <sup>4</sup>Spektor, R. and Choueiri, E., "Ion Acceleration by Beating Electrostatic Waves: Domain of Allowed Acceleration," *Phys. Rev. E*, Vol. 69, No. 4, April 2004, pp. 046402.
- <sup>5</sup>Skiff, F., Anderegg, F., and Tran, M., "Stochastic particle acceleration in an electrostatic wave," *Phys. Rev. Lett.*, Vol. 58, No. 14, April 1987, pp. 1430.
- <sup>6</sup>Alba, S., Carbone, G., Fontanesi, M., Galassi, A., Riccardi, C., and Sindoni, E., "Stochastic particle acceleration in an electrostatic wave," *Plasma Phys. Controlled Fusion*, Vol. 34, No. 2, 1992, pp. 147.
- <sup>7</sup>Spektor, R. and Choueiri, E., "Design of an Experiment for Studying Ion Acceleration by Beating Waves," Presented at the 38<sup>th</sup> AIAA/ASME/SAE/ASEE Joint Propulsion Conference (JPC), Indianapolis, Indiana, July 7-10, 2002.
- <sup>8</sup>Spektor, R. and Choueiri, E., "Excitation and propagation of Electrostatic Ion Cyclotron waves in rf-sustained plasmas of interest to propulsion research," Presented at the 40<sup>th</sup> AIAA/ASME/SAE/ASEE Joint Propulsion Conference (JPC), Fort Lauderdale, Florida, July 11-14, 2004.
- <sup>9</sup>Fasoli, A., Skiff, F., and Tran, M., "Study of wave-particle interaction from the linear regime to dynamical chaos in a magnetized plasma," *Phys. plasmas*, Vol. 1, No. 5, May 1994, pp. 1452.
- <sup>10</sup>Choueiri, E. Y., "Anomalous resistivity and heating in current-driven plasma thrusters," *Phys. Plasmas*, Vol. 6, No. 5, May 1999, pp. 2290.
- <sup>11</sup>Choueiri, E. and Spektor, R., "Coherent ion acceleration using two electrostatic waves," Presented at the 36<sup>th</sup> AIAA Joint Propulsion Conference, Huntsville, AL, July 16-20, 2000. AIAA-2000-3759.
- <sup>12</sup>Stix, T., *Waves in Plasmas*, Springer-Verlag, New York, 1992.
- <sup>13</sup>Goree, G., *The backward electrostatic ion-cyclotron wave, fast wave current drive, and fir laser scattering.*, Ph.d, Princeton University, 1985.
- <sup>14</sup>Neynaber, R., Trujillo, S., and Rothe, E., "Symmetric-Resonance Charge Transfer in Ar from 0.1–20 eV Using Merging Beams," *Phys. Rev.*, Vol. 157, No. 1, May 1967, pp. 101.
- <sup>15</sup>Scime, E., Biloiu, C., Compton, C., Doss, F., Venture, D., Heard, J., Choueiri, E., and Spektor, R., "Laser induced fluorescence in a pulsed argon plasma," *Rev. Sci. Instrum.* 76, 026107 (2005), Vol. 76, 2005, pp. 026107.
- <sup>16</sup>Biloiu, C., Sun, X., Choueiri, E., Doss, F., Scime, E., Heard, J., Spektor, R., and Ventura, D., "Evolution of the Parallel and Perpendicular

Ion Velocity Distribution Function in Pulsed Helicon Plasma Sources Obtained by Time Resolved Laser Induced Fluorescence," *To be published in Physics of Plasmas*, Vol. , pages = ,.

<sup>17</sup> Kline, J., *Resonant Ion Heating in a Helicon Plasma*, Ms, West Virginia University, 1998.

<sup>18</sup> Kline, J., Scime, E., Keiter, P., Balkey, M., and Boivin, R., "Ion heating in the HELIX helicon plasma source," *Phys.Plasmas*, Vol. 6, No. 12, December 1999, pp. 4767–4772.

<sup>19</sup> Karney, C., "Stochastic ion heating by a lower hybrid wave:II," *Phys.Fluids*, Vol. 22, No. 11, November 1979, pp. 2188.

<sup>20</sup> Spektor, R. and Choueiri, E., "Ion Acceleration by Beating Electrostatic Waves: Criteria for Regular and Stochastic Acceleration," Presented at the 27<sup>th</sup> International Electric Propulsion Conference (IEPC), Pasadena, California October 14-19, 2001. IEPC-01-209.

<sup>21</sup> Spektor, R. and Choueiri, E., "Effects of Ion Collisions on Ion Acceleration by Beating Electrostatic Waves." Presented at the 28<sup>th</sup> International Electric Propulsion Conference (IEPC), Toulouse, France March 17-21, 2003. IEPC-03-65.